Cell Insight 2 (2023) 100078

Contents lists available at ScienceDirect

Cell Insight

journal homepage: www.journals.elsevier.com/cell-insight

Research Article

A role for *Hes1* in constraining germinal center B cell formation☆

Xingxing Shao [a,b,c], Xin Liu [b,d], Hai Qi [a,b,c,d,e,f,*]

[a] Tsinghua-Peking Center for Life Sciences, Beijing, China
[b] Laboratory of Dynamic Immunobiology, Institute for Immunology, Tsinghua University, Beijing, China
[c] School of Life Sciences, Tsinghua University, Beijing, China
[d] Department of Basic Medical Sciences, School of Medicine, Tsinghua University, Beijing, China
[e] Frontiers Beijing Frontier Research Center for Biological Structure, Tsinghua University, Beijing, China
[f] Beijing Key Laboratory for Immunological Research on Chronic Diseases, Tsinghua University, Beijing, China

HIGHLIGHTS

- Removal of HES1 from B cells causes germinal center expansion.
- HES1 negatively regulates germinal center B cell formation by repressing *Bcl6* expression.
- The expression of *Hes1* is repressed by B cell receptor signaling early after activation.

GRAPHICAL ABSTRACT

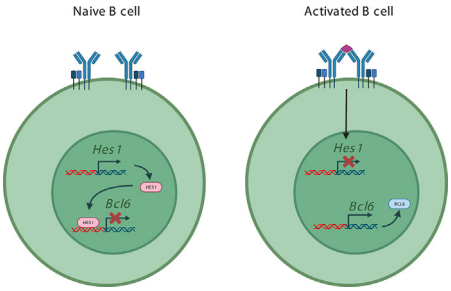

ABSTRACT

Germinal center is a transient lymphoid tissue structure in which B cells undergo affinity maturation and differentiate into memory B cells and plasma cells. GC formation depends on B cell expression of BCL6, a master transcription regulator of the GC state. Bcl6 expression is under elaborate control by external signals. HES1 plays important roles in T-cell lineage commitment, although little is known about its potential roles in GC formation. Here we report that B-cell-specific HES1 deletion causes a significant increase in GC formation, leading to increased production of plasma cells. We further provide evidence that HES1 inhibits BCL6 expression in a bHLH domain-dependent manner. Our study suggests a new layer of regulation of GC initiation mediated by HES1 and, by inference, Notch signals *in vivo*.

1. Introduction

The Notch signaling pathway is highly conserved among bilaterians, transmitting signals directly from the plasma membrane to the nucleus (Artavanis-Tsakonas et al., 1999). It not only has pleiotropic functions in diverse developmental processes, but also plays important roles in various disease conditions (Bray, 2016). The Notch receptor undergoes proteolytic cleavages upon ligand binding, releasing the Notch intracellular domain (NICD), which then translocates into the nucleus and initiates gene transcription together with other transcriptional regulators and co-activators (Bray, 2016). The target genes induced by Notch signaling is highly context-dependent, among which the HES family of genes encoding basic helix-loop-helix (bHLH) transcription factors represent the most studied ones (Iso et al., 2003). *Hes1* is the major HES family member expressed in the immune system. It is known to regulate the development and function of both innate and adaptive immune cells downstream of Notch signaling (Amsen et al., 2015; Lin et al., 2018; Wendorff et al., 2010).

Mature B cells consist of innate-like B1 cells and conventional B2 cells, and the latter can be further divided into follicular B (FoB) cells and

☆ Hai Qi is the Lead Contact for this manuscript.

* Corresponding author. Tsinghua-Peking Center for Life Sciences, Beijing, China.
E-mail address: qihai@tsinghua.edu.cn (H. Qi).

https://doi.org/10.1016/j.cellin.2023.100078
Received 28 November 2022; Received in revised form 17 January 2023; Accepted 17 January 2023
Available online 28 January 2023

marginal zone (MZ) B cells. The Notch receptor is expressed in all three subsets (Saito et al., 2003) and controls the development of MZ B cells, but not other subsets, in a *Hes1* independent manner (Wendorff et al., 2010). Although FoB cells express functional Notch receptors and upregulate *Hes1* expression upon exposure to Notch ligands (Lechner et al., 2021), biological functions of Hes1 in these cells are not fully elucidated.

During a typical T-dependent B cell response, antigen-activated FoB cells migrate to the T zone-follicle border to forge prolonged interactions with cognate T cells before developing into germinal centers (GCs) (Garside et al., 1998; Kerfoot et al., 2011; Okada et al., 2005; Qi et al., 2008), the highly dynamic lymphoid tissue microdomain that supports somatic hypermutation and affinity-based selection to give rise to high-affinity long-lived plasma cells (PCs) and memory B cells (MBCs) (Victora & Nussenzweig, 2022). Entry into GCs is tightly regulated to avoid emergence of autoimmunity and tumorigenesis (Mlynarczyk et al., 2019; Vinuesa et al., 2009). The expression of *Bcl6*, the master transcriptional regulator of GC B cell identity, is essential for GC entry (Basso & Dalla-Favera, 2012). Previous studies have shown that the upregulation of *Bcl6* is promoted by binding of MEF2B to its promoter region, and requires *Irf4* expression downstream of BCR activation (Song & Matthias, 2018). However, the complete regulatory network controlling *Bcl6* expression is not fully elucidated.

Here we show that *Hes1* expression in FoB cells is negatively regulated by BCR signaling, and *Hes1* restrains GC commitment by repressing *Bcl6* upregulation. Conditional removal of the *Hes1* gene from the B-lineage cells exaggerated GC response both at the steady state and upon immunization with foreign antigens. Our results identify *Hes1* in B cells and, by inference, Notch signaling inside the follicle as a regulatory pathway that constrains GC development.

2. Results

2.1. Conditional Hes1 deletion in B cells leads to GC expansion

Compared to naïve B cells, the mRNA and protein levels of *Hes1* is greatly reduced in GC B cells (Fig. 1a). This appears to be an event directly associated with B cell receptor (BCR) signaling, since naïve B cells downregulated both the *Hes1* transcript and protein in response to BCR stimulation *in vitro* (Fig. 1b). To investigate whether the expression of *Hes1* in B cells might limit GC response, we constructed a *Cd79a*-cre *Hes1*$^{fl/fl}$ mouse model, which conditionally deletes *Hes1* from B cells (Fig. 1c). Flow cytometry analyses of different early B cell precursors in the bone marrow (Fig. S1a) showed that B cell development is grossly normal in these mice compared to the *Cd79a*-cre *Hes1*$^{+/+}$ control animals (Fig. S1b). However, spontaneously formed GC B cells is more abundant in these animals at the steady state (Fig. 1d and e), suggesting that HES1 might negatively regulate GC reaction in B cells. Next, we intraperitoneally immunized *Cd79a*-cre *Hes1*$^{+/+}$ and *Hes1*$^{fl/fl}$ mice with NP-KLH (4-hydroxy-3-nitrophenylacetyl hapten conjugated to keyhole limpet haemocyanin), and examined the abundance of NP-specific GC B cells at the early (day 7), peak (day 14) and late (day 28) time points post immunization (Fig. 1f). We found that both the total and NP-specific GC B cells are significantly increased in the *Hes1*$^{fl/fl}$ mice compared to the control animals at all time points analyzed (Fig. 1g). Consistent with these findings, immunohistochemistry analysis also showed that splenic GCs, as revealed by the EFNB1 staining, were significantly enlarged in the *Hes1*$^{fl/fl}$ animals 7 days post immunization (Fig. 1h). On the other hand, affinity maturation, as measured by the fraction of the NP-specific V_H186.2 clones that carried the affinity-enhancing W33L mutation, is not detectibly disturbed in *Hes1* deficient GC B cells (Fig. 1i). Taken together, these results indicate that *Hes1* deletion in B cells encourages GC reaction.

To more specifically examine the function of *Hes1* in regulating GC response, we constructed a *S1pr2*-creERT2 *Hes1*$^{fl/fl}$ mouse model carrying a loxP-STOP-loxP-tdTomato (Ai14) allele, which allows inducible *Hes1* deletion and tdTomato expression in activated pre-GC as well as GC B cells (Shinnakasu et al., 2016; Viant et al., 2021). The mice were intraperitoneally immunized with NP-KLH and gavaged with 2 mg tamoxifen every two days, starting from 6 days post immunization, to induce *Hes1* deletion. We performed FACS analyses 14 days post immunization to measure the abundances of tdTomato $^{+}$ GC as well as the GC-experienced tdTomato^{+} plasma cells (PCs) and memory B cells (MBCs) in the spleen of these animals (Fig. 2a and b). Our results showed that the percentages of GC B cells were significantly increased in the *Hes1*$^{fl/fl}$ mice compared to the *Hes1*$^{+/+}$ control animals (Fig. 2c), Indicating that *Hes1* functioned in activated B cells that were either ready to adopt or have already adopted the GC identity. On the other hand, GC-derived MBCs remained unchanged in the *Hes1*$^{fl/fl}$ mice (Fig. 2d), while PCs slightly increased (Fig. 2e), arguing against a defect in post-GC cell fate decisions. To more specifically rule out a role for *Hes1* in GC output, we performed another set of experiments, in which NP-KLH immunized *S1pr2*-creERT2 Ai14 *Hes1*$^{+/+}$ and *Hes1*$^{fl/fl}$ mice were treated with tamoxifen on day 9, 10 and 11 post immunization, well after the establishment of GCs. Abundances of tdTomato^{+} GC B cells, MBCs and PCs were analyzed a day after the last dose of tamoxifen (Fig. S2a). Under such conditions, we found that all three populations remained the same between the *Hes1*$^{+/+}$ and *Hes1*$^{fl/fl}$ mice (Fig. S2b-d). Taken together, these results suggest that *Hes1* likely plays a negative regulatory role in the early phase of GC reaction, without affecting MBC and PC output.

2.2. Hes1 deficiency does not affect GC B cell proliferation or apoptosis

Although *Hes1* is greatly downregulated in GC B cells, the residue protein expressed could still play a regulatory role (Fig. 1a), restricting the size of GCs by limiting cell proliferation or enhancing apoptosis (Yoon et al., 2009). To test these possibilities, we intraperitoneally immunized *Cd79a*-cre *Hes1*$^{+/+}$ and *Hes1*$^{fl/fl}$ mice with NP-KLH, and analyzed their splenic GC B cells 7 days post immunization (Fig. S3a). We found that *Hes1* deficient GC B cells proceeded into the S phase of cell cycle at a similar speed as the wildtype GC B cells, measured by the percentage of cells incorporating BrdU within a 2-h time window (Fig. S3b). In addition, we performed intracellular staining of active caspase to measure the fraction of GC B cells undergoing apoptosis, and detected no difference between the two groups (Fig. S3c). Therefore, our results indicate that the GC expansion seen in the *Cd79a*-cre *Hes1*$^{fl/fl}$ mice was not due to altered B cell proliferation or survival in established GCs, but likely resulted from altered molecular events early in the response.

2.3. Hes1 deletion promotes early GC commitment

To determine whether *Hes1* plays a role in early GC responses, we took advantage of an adoptive transfer system that allows induction of GCs from B1-8^{hi} B cells that are specific for the hapten NP. Briefly, *Cd79a*-cre *Hes1*$^{+/+}$ and *Hes1*$^{fl/f}$ B1-8^{hi} cells were mixed and co-transferred into congenically marked CD45.1 recipients together with OT-II T cells recognizing ovalbumin (OVA). The mice were subsequently immunized with NP-OVA, and the proportion of B1-8^{hi} cells that upregulated the GC surface marker GL7 were assessed 48, 72 and 96 h after immunization (Fig. 3a). In any single experiment, either the *Hes1*$^{+/+}$ or *Hes1*$^{fl/f}$ mice carried a loxP-STOP-loxP-GFP (Ai3) allele, which helped distinguish the cells from these mice by GFP expression (Fig. 3b). To compare the likelihood of the two types of cells to become GC B cells, a competitive competency index was calculated by normalizing the ratio of *Hes1*$^{fl/fl}$ and *Hes1*$^{+/+}$ GL7^{+} cells to the ratio of total transferred B1-8^{hi} cells (Fig. 3c), and an index above 1 would indicate relative advantage gained by *Hes1*$^{fl/fl}$ GL7^{+} cells. Both *Hes1*$^{+/+}$ and *Hes1*$^{fl/fl}$ B1-8^{hi} cells are equally capable of upregulating GL7 as soon as 48 h post immunization, with a competitive competency index around 1. However, the *Hes1*$^{fl/fl}$ cells started to gain advantage at 72 h post immunization, and the difference was further enlarged 24 h later (Fig. 3c). To determine whether this was due to differences in cell proliferation, we stained B cells with cell trace violet

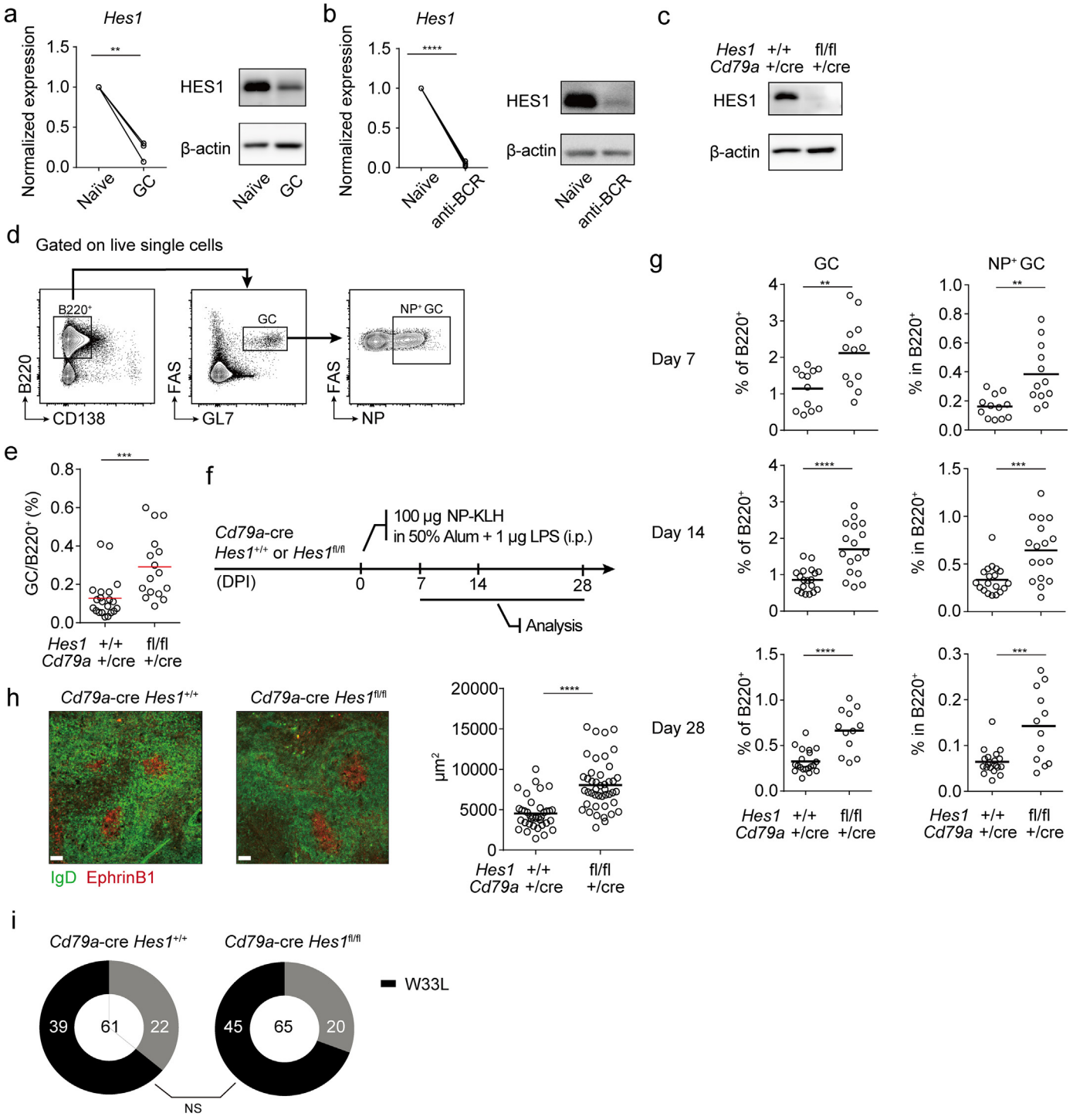

Fig. 1. Conditional *Hes1* deletion in B cells leads to GC expansion. (a) Quantitative PCR (qPCR) and western blotting were performed to measure *Hes1* transcript (left) and protein (right) levels in naïve or GC B cells. (b) Levels of *Hes1* transcript (left) and protein (right) in naïve or BCR-stimulated B cells. Cells were treated with 5 μg/ml anti-IgM F(ab')$_2$ antibodies and analyzed 24 h later. qPCR results were first normalized to the level of *Actb* (a and b) then to the naïve cells. Data are pooled from three (a) or four (b) independent experiments. Each symbol indicates the mean from one experiment. (c) Knockout efficiency of Hes1 in the *CD79a*-cre *Hes1*$^{fl/fl}$ naïve B cells measured at the protein level. Data are representative of two independent experiments. (d–h) GC reaction in *CD79a*-cre *Hes1*$^{+/+}$ and *Hes1*$^{fl/fl}$ mice at steady state and upon intraperitoneal (i.p.) NP-KLH immunization. (d) Gating strategies. (e) Quantifications of spontaneous splenic GCs in unimmunized *CD79a*-cre *Hes1*$^{+/+}$ and *Hes1*$^{fl/fl}$ mice. (f) Experimental setup and immunization schedule. DPI, days post immunization. (g) Summary statistics for total and NP-specific GC B cells in the spleen of *CD79a*-cre *Hes1*$^{+/+}$ and *Hes1*$^{fl/fl}$ mice at indicated time points post immunization. Data are pooled from at least two independent experiments, with at least three animals analyzed in each experiment. Each symbol indicates one mouse, and lines denote means. (h) Immunohistochemistry staining (left) and summary statistics (right) of GC areas in the splenic sections from the *CD79a*-cre *Hes1*$^{+/+}$ and *Hes1*$^{fl/fl}$ mice 7 days post NP-KLH immunization (i.p). Scale bar denotes 50 μm. Each symbol denotes one GC, and data are pooled from three mice per group. (i) Pie charts showing the fraction of V_H186.2 GC B cells carrying the W33L mutation. Cells were isolated from the *CD79a*-cre *Hes1*$^{+/+}$ and *Hes1*$^{fl/fl}$ mice, respectively, 28 days post NP-KLH immunization. Numbers of the total sequences analyzed as well as sequences with or without the W33L mutation are shown. Data are pooled from three independent experiments. *P* values by student's *t*-test (a, b, e, g and h) or two-tailed Fisher's exact test (i). *, $P < 0.05$; **, $P < 0.01$; ***, $P < 0.001$; ****, $P < 0.0001$; NS, not significant.

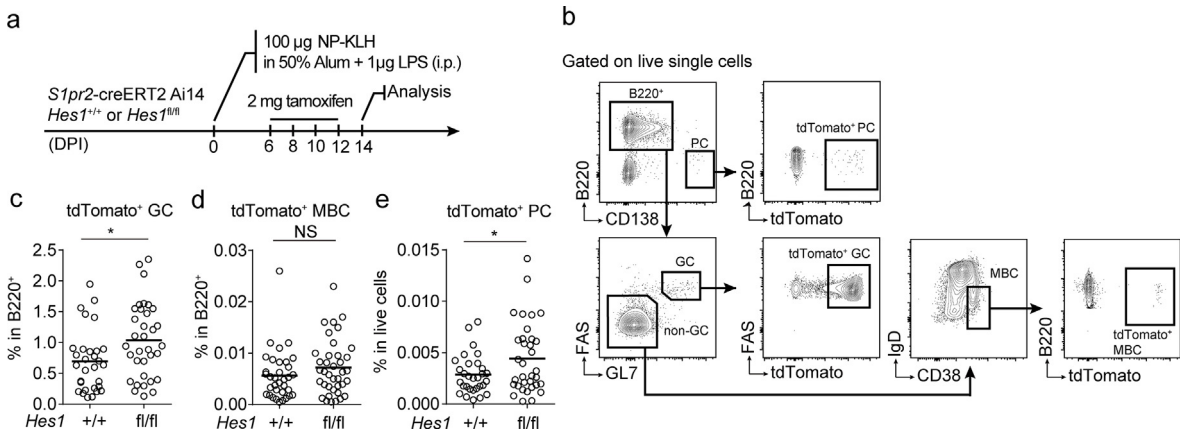

Fig. 2. Inducible deletion of *Hes1* in GC B cells enhances GC reaction. (a) Experimental schedule. *S1pr2*-creERT2 Ai14 *Hes1*$^{+/+}$ and *Hes1*$^{fl/fl}$ mice were immunized intraperitoneally with NP-KLH and gavaged with tamoxifen every two days, starting from 6 days post immunization. FACS analyses of splenocytes were performed two weeks after immunization. (b) Gating strategies. (c–f) Summary statistics showing the abundances of tdTomato^{+} GC(c), MBC (d) and PC(e) in *S1pr2*-creERT2 Ai14 *Hes1*$^{+/+}$ and *Hes1*$^{fl/fl}$ mice. Data are pooled from six independent experiments, with at least three mice per group. Each symbol indicates one mouse, and lines denote means. *P* values by student's *t*-test. *, $P < 0.05$; NS, not significant.

(CTV) prior to the transfer, and measured cell expansion by the dilution of the dye. Our results showed that the proliferation of *Hes1*$^{+/+}$ and *Hes1*$^{fl/fl}$ B1-8^{hi} are comparable both at 48 and 72 h post immunization (Fig. S4a and b). Furthermore, B cells isolated from *Cd79a*-cre *Hes1*$^{+/+}$ and *Hes1*$^{fl/f}$ mice mounted similar calcium responses upon BCR stimulation (Fig. S4c), ruling out the role of *Hes1* in regulating B cell activation. Collectively, these results indicate that *Hes1* functions by repressing early B cell commitment to the GC reaction.

2.4. HES1 represses Bcl6 expression

The upregulation of *Bcl6* in B cells is important for initiating GC reaction (Robinson et al., 2020), and previous studies have reported that over-expression of the NICD represses *Bcl6* expression in follicular B cells (Zhang et al., 2013). Therefore, we tested whether *Hes1* deficiency increases the level of *Bcl6* in early GC B cells. To do that, we performed adoptive transfer experiments as described above, and sorted either FAS^{-}GL7^{-} or GL7^{+} subsets of *Hes1*$^{fl/fl}$ and *Hes1*$^{+/+}$ B1-8^{hi} cells from immunized mice 72 h post immunization. For both subsets analyzed, the mRNA level of *Bcl6* was significantly higher in the *Hes1*$^{fl/fl}$ cells compared to the *Hes1*$^{+/+}$ control (Fig. 3d), indicating that *Hes1* inhibited *Bcl6* upregulation in B cells. To test whether HES1 also plays a role in regulating *Bcl6* levels in naïve or established GC B cells, we sorted both of the populations from the spleen of *CD79a*-cre *Hes1*$^{+/+}$ and *Hes1*$^{fl/fl}$ mice 14 days post intraperitoneal NP-KLH immunization, and found no difference in the abundances of *Bcl6* transcripts between the two groups (Fig. S5a). Consistent with these results, the protein level of BCL6 was not different between *Hes1*$^{+/+}$ and *Hes1*$^{fl/fl}$ GC B cells, as quantified by FACS analyses (Fig. S5b). Taken together, these results indicate that HES1 negatively regulates *Bcl6* expression at the early stage of GC reaction.

To further confirm these results, we over-expressed *Hes1* in induced GC-like B cells (iGB) cultured *in vitro* (Nojima et al., 2011), and measured *Bcl6* transcription level in these cells. Consistent with what we observed *in vivo*, the level of *Bcl6* was significantly downregulated in *Hes1* over-expressed cells compared to the empty vector control (Fig. 4a), further supporting the role of *Hes1* in repressing Bcl6 expression. Next, we sought to determine the mechanism of such regulation. Based on the prediction provided by the JASPAR database, multiple HES1 binding sites were found within the *Bcl6* promoter region (Fig. 4b). We thus performed a luciferase reporter assay to test whether HES1 directly regulates *Bcl6* transcription. Briefly, a construct containing firefly luciferase driven by the *Bcl6* promoter was transfected into 293T cells together with either an empty vector, wildtype HES1, or a truncated mutant lacking the basic helix-loop-helix (bHLH) DNA binding domain, and the luciferase activity was measured 48 h post transfection. Compared to the empty vector control, expression of wildtype HES1 but not the bHLH-truncated mutant significantly repressed luciferase expression (Fig. 4c). Taken together, our results indicate that HES1 directly suppress *Bcl6* transcription, likely through binding to its promoter region.

3. Discussion

Notch signaling is known to regulate the development of both T cells and marginal zone B cells (Bray, 2016). It is also involved in guiding effector T cell differentiation (Amsen et al., 2015). The Notch receptor and ligand is expressed abundantly by B cells (Lechner et al., 2021) and follicular stroma cells (Santos et al., 2007), respectively. Ligand binding to the Notch receptor in B cells are found to have a synergistic effect with CD40, toll-like receptor or BCR stimulation to promote B cell activation, class-switching and antibody secretion (Santos et al., 2007; Thomas et al., 2007), however, the role of the Notch signaling pathway in GC response remained incompletely understood. Here we show that *Hes1*, a well-characterized Notch target gene, is involved in regulating *Bcl6* expression and GC reaction in B cells. The expression of *Hes1* is down-regulated by BCR stimulation in B cells (Fig. 1b) in addition to being controlled by Notch signaling (Lechner et al., 2021), suggesting potential crosstalk between the two pathways. These findings have also added more complexity to the known signaling network controlling GC commitment, and indicates that BCR signaling promotes *Bcl6* upregulation by repressing a negative regulatory component.

We found that the removal of *Hes1* from the B-lineage cells leads to expansion of both spontaneous and immunization-induced GCs (Fig. 1d and f), without affecting GC competition or post-GC differentiation (Figs. 1g and Fig. 2c–e). Consistent with these results, the *Hes1* deficiency also has no effect on the *Bcl6* expression level in established GC B cells (Fig. S4). Instead, it actively suppresses upregulation of *Bcl6* at the early GC commitment stage (Fig. 3c and d). The lack of function of *Hes1* in GC B cells could be explained by its downregulation in these cells (Fig. 1a); alternatively, the transcriptional remodeling in GC B cells might decouple *Hes1* from regulating *Bcl6* expression. The upregulation of *Bcl6* is known to be induced at the T-B border in pre-GC B cells, shortly after antigen engagement (Robinson et al., 2020). Therefore, our results support a model in that GC precursors with higher affinities have a stronger tendency to downregulate *Hes1* and release the suppression of *Bcl6*. This is consistent with the observation that high affinity B cells have a relative

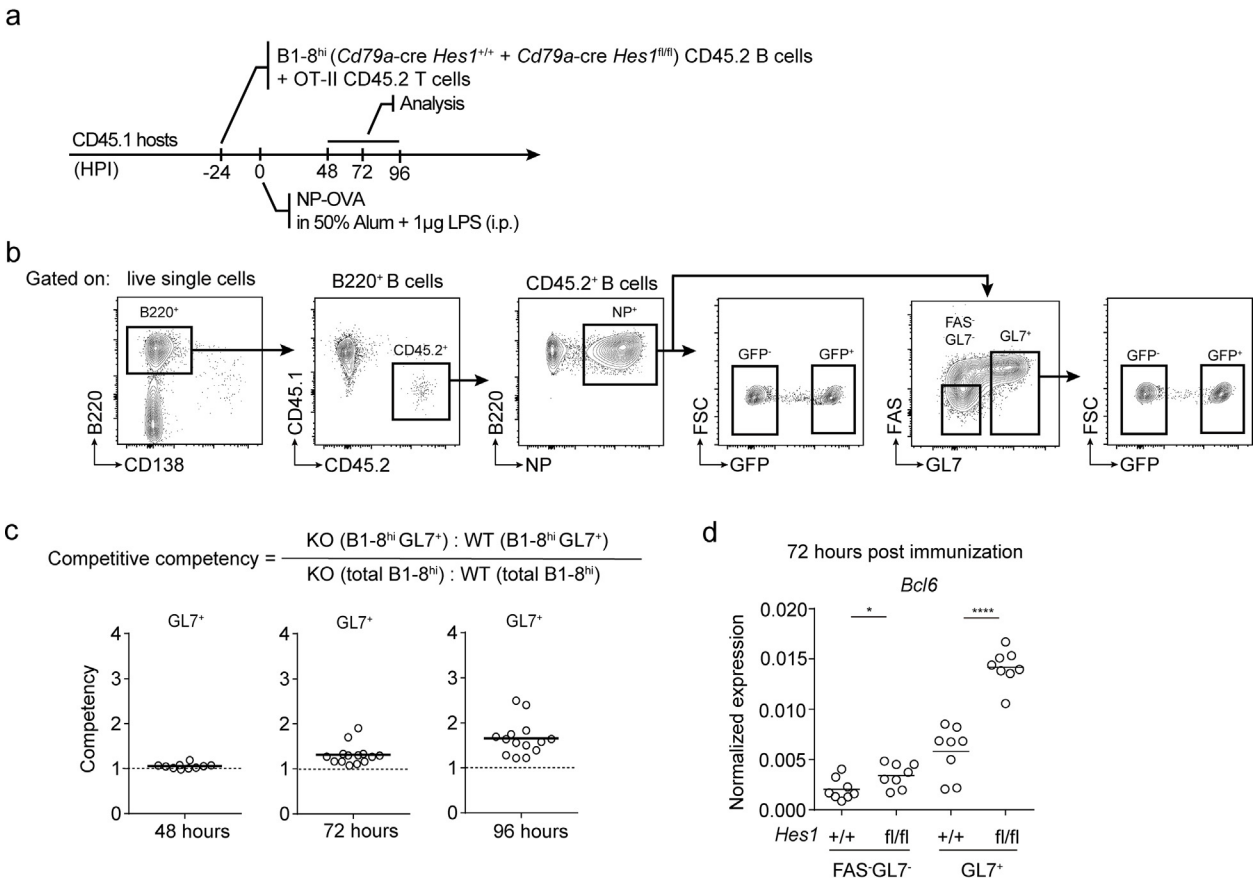

Fig. 3. HES1 negatively regulates GC initiation. (a) Experimental setup. A mix of 3×10^5 B1-8^{hi} *Cd79a*-cre *Hes1*$^{+/+}$ B cells, 3×10^5 B1-8^{hi} *Cd79a*-cre *Hes1*$^{fl/fl}$ B cells and 6×10^5 OT-II T cells were transferred into CD45.1 congenic recipients 24 h prior to NP-OVA immunization. FACS analyses of splenocytes were performed at indicated time points post immunization. In each experiment, either the *Hes1*$^{+/+}$ or *Hes1*$^{fl/fl}$ mice carried an Ai3 allele, allowing the identification of the two genotypes by GFP expression. (b) Gating strategies. (c) Competitive competency of B1-8^{hi} *Cd79a*-cre *Hes1*$^{+/+}$ and *Hes1*$^{fl/fl}$ GL7$^+$ cells was calculated by normalizing the ratio of these cells to the ratio of total B1-8^{hi} *Hes1*$^{+/+}$ and *Hes1*$^{fl/fl}$ cells (upper panel), and summary statistics are shown (lower panel). Data are pooled from at least four independent experiments with at least two mice per group. Each symbol indicates one mouse, and lines denote means. (d) Summary statistics of *Bcl6* mRNA levels in the FAS$^-$GL7$^-$ and GL7$^+$ populations sorted from transferred B1-8^{hi} *Cd79a*-cre *Hes1*$^{+/+}$ and *Hes1*$^{fl/fl}$ cells 72 h post immunization, normalized to the level of *Actb*. Data are pooled from four independent experiments, and two independently sorted samples are included in each experiment. Each symbol indicates measurement from one sorted sample, lines denote means. *P* values by student's *t*-test. *, $P < 0.05$; ****, $P < 0.0001$.

advantage in joining GC reaction (Schwickert et al., 2011; Yeh et al., 2018).

Although we have not defined precisely how BCR signaling represses *Hes1* expression, a growing body of evidence suggests that *Hes1* can be regulated in a Notch-independent manner. For example, *Hes1* expression is modulated by the nuclear factor kappa B (NF-kB) and c-jun N-terminal protein kinase (JNK) pathways (Curry et al., 2006; Zhao et al., 2018), both known to be downstream of BCR signaling (Efremov et al., 2020). In addition, it was shown that Ikaros, a transcription factor widely expressed by lymphocyte and activated by antigen receptor signaling (Kathrein et al., 2008; Ma et al., 2013), specifically represses *Hes1* expression (Kathrein et al., 2008). The coupling of antigen receptor signaling and the Notch pathway components might help B cells to better coordinate these pathways.

Spontaneous GCs can be found in autoimmune-prone mice as well as specific pathogen free animals (Luzina et al., 2001; Soni et al., 2014), and often contain self-reactive B cells (Domeier et al., 2017). The increase representation of these cells in the *Hes1* deficient animals suggests that *Hes1* might restrain autoreactive B cells from entering GC reaction, thus potentially preventing the onset of autoimmune diseases. Further investigations are needed to reveal whether altered *Hes1* activity in B cells contribute to autoimmunity.

In summary, our results reveal a negative regulatory role for *Hes1* in B cell commitment to the GC reaction. These findings will help us further understand the role of Notch signaling in humoral immune response and autoimmune diseases.

4. Materials and methods

4.1. Mice

C57BL/6J (Jax 664), CD45.1 (Jax 2014), Ai3 (Jax 7903), Ai14 (Jax 7914) and OVA323-339-specific TCR transgenic OT-II (Jax 4194) mice were originally from the Jackson Laboratory. The *Hes1*$^{fl/fl}$ strain was a gift from Dr. Xiaoyu Hu; the *Cd79a*-cre strain was from Dr. Michael Reth; the B1-8^{hi} strain was from Dr. Michel C. Nussenzweig; and the *S1pr2*-creERT2 strain was from Dr. Tomohiro Kurosaki. All animals were maintained under the specific pathogen-free conditions on a 12-h light-dark cycle at 22–26 °C and humidity at 40%–70%. All animal experiments were performed according to the governmental and institutional guidelines for animal welfare and approved by the IACUC at Tsinghua University.

4.2. Immunization, tamoxifen treatment and flow cytometry

Mice were intraperitoneally immunized with 100 μg NP-OVA or NP-KLH emulsified in the Alum Adjuvant (Invitrogen) with 1 μg LPS (Sigma). For BrdU labelling, the mice were intraperitoneally injected with 4 mg

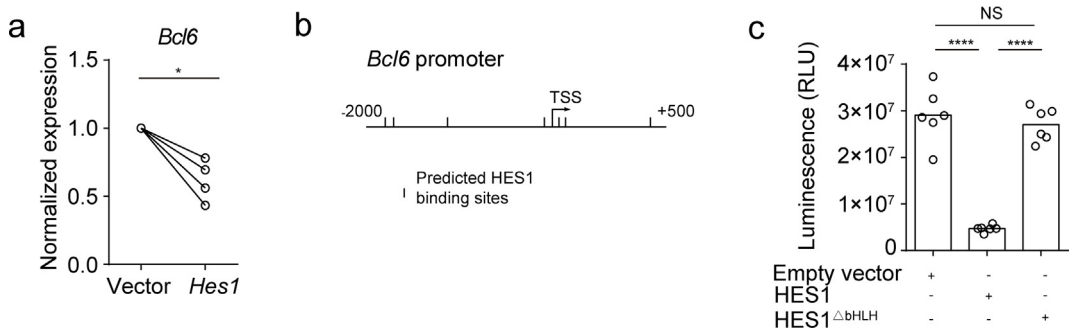

Fig. 4. HES1 suppresses *Bcl6* expression. (a) Levels of *Bcl6* transcripts in *Hes1* overexpressed iGC B cells. Results were normalized to the level of *Actb* and to the control samples. Each symbol indicates the mean value from one experiment. Data are pooled from four independent experiments. (b) A schematic diagram of the *Bcl6* promoter. Predicted HES1 binding sites are labeled (data obtained from the Jaspar database). TSS, transcription start site. (c) *Bcl6* promoter activity measured by a luciferase reporter assay (see Methods for more details). Either wildtype HES1 or HES1$^{\triangle bHLH}$, a truncated mutant without the bHLH domain, were used in the assay, and the results were compared to the empty vector control. Data are representative of three independent experiments. Each symbol indicates an experimental replicate. RLU, relative light unit. *P* values by paired student's *t*-test (a) or student's *t*-test (c). *, $P < 0.05$; ****, $P < 0.0001$; NS, not significant.

BrdU 2 h prior to the analyses. For the inducible deletion of *Hes1*, the mice were gavaged with 2 mg tamoxifen (Sigma) dissolved in corn oil (Sigma) at a concentration of 10 mg/mL, at the interval indicated.

Single cell suspension of splenocytes was incubated with 10 μg/mL 2.4G2 antibodies (BioXcell) in MACS buffer (PBS supplemented with 1% FBS and 5 mM EDTA) for 20 min before the staining. Cells were then incubated with surface staining reagents on ice for 30 min, washed twice, and resuspended in MACS buffer for analyses. To measure BCL6 expression in GC B cells, cells were additionally fixed and permeablized using the Foxp3 Transcription Factor Staining kit (eBioscience), and stained with anti-BCL6 antibodies for 90 min on ice. Staining reagents used include APC-cy7-anti-B220 (RA3-6B2), PE-cy7-anti-CD95 (Jo2), APC-anti-CD138 (281-2), AF647-anti-BCL6 (K112-91) from BD Biosciences; AF700-anti-CD38 (90), ef450-anti-GL7 (GL-7), biotin-anti-GL7 (GL-7), biotin-anti-CD43 (eBioR2/60), PE-anti-ENPEP (6C3), ef450-anti-IgM (eB121-15F9), APC-anti-IgD (11-26c), FITC-anti-IgD (11-26c) from eBioscience; zombie yellow, APC-anti-CD45.1 (A20), percp-cy5.5-anti-CD45.1 (A20), percp-cy5.5-anti-Gr-1 (RB6-8C5), biotin-anti-CD8 (53-6.7), biotin-anti-CD4 (GK1.5), percp-cy5.5-anti-F4/80 (BM8), percp-cy5.5-anti-CD3 (17A2), AF647-anti-CD45.2 (104), FITC-anti-CD24 (M1/69), APC-streptavidin, APC-cy7-streptavidin, APC-cy7-anti-CD45.2 (104) from BioLegend and NP-PE from Biosearch Technologies. Staining of BrdU (FITC-BrdU flow kit, BD) and active caspase (CaspGLOW fluorescein active caspase staining kit, Invitrogen) were performed according to the manufacturer's instructions. Data were collected on a LSR II or an Aria III (BD) flow cytometer, and analyzed with the FlowJo software (TreeStar).

4.3. Cell isolation, CTV staining and adoptive transfer

For the adoptive transfer experiments, B cells were isolated from the spleens of B1-8^{hi} *Cd79a*-cre *Hes1*$^{+/+}$ and *Hes1*$^{fl/fl}$ mice by negative selection. Briefly, splenocytes were incubated with an antibody cocktail containing biotin-anti-CD43 (eBioR2/60), biotin-anti-CD4 (GK1.5), biotin-anti-CD3 (17A2), biotin-anti-CD8 (53-6.7) antibodies for 30 min on ice, washed, and isolated by using the anti-biotin Microbeads (Miltenyi Biotec) according to the manufacturer's instructions. Splenic CD4 T cells were isolated from the OT-II mice by using the CD4 Microbeads (Miltenyi Biotec). Approximately 3×10^5 *Hes1*$^{+/+}$ B1-8^{hi} B cells, 3×10^5 *Hes1*$^{fl/fl}$ B1-8^{hi} B cells and 6×10^5 OT-II T cells were mixed and transferred into CD45.1 recipients. The mice were immunized intraperitoneally with NP-OVA 24 h later and analyzed at the indicated time points. In each experiment, either the *Hes1*$^{+/+}$ or *Hes1*$^{fl/fl}$ donor carried a Ai3 allele, allowing the gating of the two types of cells, and summary statistics were pooled from both conditions. In experiments measuring cell proliferation, B1-8^{hi} cells were stained with 5 μM Cell Trace Violet (Invitrogen) in PBS at 37 °C for 12 min, washed twice with RPMI medium before being transferred.

4.4. iGC B cell culture and retroviral transduction

The open reading frame of *Hes1* was cloned into a MSCV retroviral vector that also expresses GFP under the control of the human ubiquitin C promoter. The *Hes1* or the empty control vector were transfected into the Platinum-E packaging cell line, and the viral supernatants were collected 48 h later.

iGC B cells were induced and cultured as described (Nojima et al., 2011). Briefly, B cells were isolated by negative selection as described above, and plated onto 3T3 feeder cells expressing both CD40L and BAFF (B cell activating factor) and pre-treated with 10 μg/mL mytomycin C (Sigma). Cells were cultured in complete RPMI medium with 1 ng/mL IL-4 (peprotech). B cells were collected and spinfected twice with the indicated viral supernatants 24 and 48 h afterwards, at 1500×*g* and in the presence of 4 μg/mL polybrene (Sigma), for 2 h at 32 °C. The infected B cells were sorted 48 h post infection for qPCR analyses.

4.5. Immunohistochemistry

Staining of splenic sections were done as previously described (Qi et al., 2006). Briefly, spleens were fixed in periodate-lysine-paraformaldehyde fixative for 12 h followed by dehydration in 30% sucrose overnight. Samples were subsequently embedded and frozen in O.C.T. compound (Sakura), and sliced into 14 μm sections. The sections were first blocked in 0.1 M Tris-HCl buffer with 0.3% Triton and 1% FBS, then stained with eFlour450-anti-IgD (11-26c, ebioscience) and polyclonal goat-anti-mouse EFNB1 (R&D), followed by AlexaFluor 647 conjugated donkey anti-goat IgG secondary antibodies (Invitrogen).

4.6. In vitro calcium assay

Splenic B cells were positively isolated by using the CD19 Microbeads (Miltenyi Biotec) from *Cd79a*-cre *Hes1*$^{+/+}$ and *Hes1*$^{fl/fl}$ mice, and cultured in complete RPMI medium containing 5 μg/mL anti-IgM F(ab')$_2$ antibodies (Jackson ImmunoResearch) for 3 days. Subsequently, cells were stained with 2 mM Indo-1 (Invitrogen) in RPMI medium at a density of 10^7 per ml at 37 °C for 30 min, washed twice with ice-cold RPMI medium containing 1% serum, and resuspended in 300 μL pre-warmed RPMI medium for FACS analyses. Data were recorded for 1 min, and 10 μg/mL anti-IgM F(ab')$_2$ antibodies were added to the cells before data recording resumed for another 4 min.

4.7. Quantitative PCR

The analyses in Fig. 3d were performed according to the Smart-seq2 protocol (Picelli et al., 2014). Briefly, 200 cells were sorted directly into lysis buffer, and first strand cDNA synthesis were carried out by using the folling primers: Oligo-dT30VN (5'-AAGCAGTGGTATCAACGCAGAGTACT30VN-3'), TSO(5'-AAGCAGTGGTATCAACGCAGAGTACATrG rG + G-3'). The reverse-transcribed cDNA were subsequently amplified with the ISPCR primer (5'-AAGCAGTGGTATCAACGCAGAGT-3') and subjected to qPCR analyses. For bulk qPCR analyses, total RNA was extracted from the sorted cells by the RNeasy PlusMini or Micro Kit (QIAGEN) and then reverse-transcribed using the 5 × All in one Kit (Applied Biological Materials). qPCR reactions were performed using 2 × qPCR MasterMix (Applied Biological Materials) and data were collected by the **CFX96** detection system (Bio-Rad). Primers used include: *Actin* sense 5′-ACACCCGCCACCAGTTCGC-3′, *Actin* antisense 5′-ATGGGGTACTTCAGGGTCAGGATA-3′; *Hes1* sense 5′-GTCAACAC GACACCGGACAA-3′, *Hes1* antisense 5′-AATGCCGGGAGCTATCTT TCTT-3′; *Bcl6* sense 5′-TAGAGCCCATAAGACAGTGCT-3′, *Bcl6* antisense 5′-CACCGCCATGATATTGCCTTC-3′; *Cd19* sense 5′-AAATCCACGC ATTCAAGTC-3′, *Cd19* antisense 5′- TTCTCATAGCCACTCCC ATCC-3′.

4.8. Western blotting

Freshly isolated B cells were directly lysed with the RIPA lysis buffer (beyotime), or cultured in complete RPMI medium containing 5 μg/mL anti-IgM F(ab')$_2$ for 24 h before the lysis. Cells were incubated in lysis buffer for 10 min on ice and centrifuged at 16,000 g for 10 min at 4 °C to remove cell debris. Subsequently, protein lysates were mixed with 5 × SDS-PAGE loading buffer (beyotime) and boiled at 100 °C for 10 min before the gel electrophoresis. Antibodies used are anti-HES1 (Cell Signaling Technology), anti-β-actin (Easybio) and goat anti-rabbit IgG-HRP (Easybio).

4.9. Analyses of the V_H186.2 sequences

Live single NP-specific B220$^+$GL7$^+$ FAS$^+$ GC B cells were isolated and sorted from the spleens of *Hes1*$^{+/+}$ and *Hes1*$^{fl/fl}$ mice 28 days post NP-KLH immunization as previously described (Shi et al., 2018). Briefly, two hundred cells were sorted directly into each tube containing lysis buffer, and the cells were subsequently incubated at 65 °C for 5 min, followed by reverse-transcription with the Superscript cDNA Synthesis Kit (Invitrogen) according to the manufacturer's instructions. Primers used to amplify the V_H186.2 fragments are as follows: sense_1, 5′-CTCTTCTTGGCAGCAACAGC-3′, antisense_1: 5′-GCTGCTCAGAGTG TAGAGGTC-3′; sense_2, 5′-GTGTCCACTCCCAGGTCCAAC-3′; anti-sense_2, 5′-GTTCCAGGT CACTGTCACTG-3′. PCR products (~400bp in size) were purified by gel electrophoresis, cloned into the pMD-18T vector (Takara) and transformed into DH5α (Solarbio). Single bacterial colonies were sent for sequencing, and unique V_H186.2 sequences were compiled and analyzed for the W33L affinity-enhancing mutation.

4.10. Dual luciferase reporter assay

The *Hes1* open reading frame was amplified and cloned into the pHAGE lentivral vector using the following primers: *Hes1* sense (5′-ATGCCAGCTGATATAATG-3′) and *Hes1* antisense (5′- TCAGTTCCGC-CACGGTC-3'). For the bHLH truncated mutant, amino acids EHRKSSK-PIMAARRAARINESLSQLKTLILDALKKDSSRHSKLEKADILEMTVKHLRNL QRAQ were removed from the wildtype *Hes1*. A fragment (around 2500 bp in size) from the *Bcl6* promoter was amplified and cloned into the pGL3 plasmid upstream of the firefly luciferase with the following primers: *Bcl6* sense (5′-CAAAGTCACCGTGTCTTTG-3′) and *Bcl6* anti-sense (5′-TACAGTGGGAGAGACGTGG-3′). The above plasmids were transfected into 293T cells as indicated. Cells were collected and lysed 48 h post transfection, and the activity of the firefly luciferase were measured according to the manufacturer's instructions (Promega).

Author contributions

H.Q. conceptualized and supervised the study. X.S. conducted all the experiments. X.L. helped with data interpretation. All authors wrote the paper together.

Declaration of competing interest

The authors declare no competing financial interests.

Acknowledgements

We thank Dr. M. Nussenzweig for providing the B1-8^{hi} mice, Dr. Xiaoyu Hu for providing the Hes1$^{fl/fl}$ mice, Dr. M. Reth for providing the *Cd79a*-Cre mice. This work was funded by National Natural Science Foundation of China (grant No. 81621002, 81761128019, 32130037), and the Tsinghua-Peking Center for Life Sciences. Graphical abstract was created with BioRender.com.

Appendix A. Supplementary data

Supplementary data related to this article can be found at https://doi.org/10.1016/j.cellin.2023.100078.

References

Amsen, D., Helbig, C., & Backer, R. A. (2015). Notch in T Cell differentiation: All things considered. *Trends in Immunology, 36*, 802–814.
Artavanis-Tsakonas, S., Rand, M. D., & Lake, R. J. (1999). Notch signaling: Cell fate control and signal integration in development. *Science, 284*, 770–776.
Basso, K., & Dalla-Favera, R. (2012). Roles of BCL6 in normal and transformed germinal center B cells. *Immunological Reviews, 247*, 172–183.
Bray, S. J. (2016). Notch signalling in context. *Nature Reviews Molecular Cell Biology, 17*, 722–735.
Curry, C. L., Reed, L. L., Nickoloff, B. J., Miele, L., & Foreman, K. E. (2006). Notch-independent regulation of Hes-1 expression by c-Jun N-terminal kinase signaling in human endothelial cells. *Laboratory Investigation, 86*, 842–852.
Domeier, P. P., Schell, S. L., & Rahman, Z. S. (2017). Spontaneous germinal centers and autoimmunity. *Autoimmunity, 50*, 4–18.
Efremov, D. G., Turkalj, S., & Laurenti, L. (2020). Mechanisms of B Cell receptor activation and responses to B cell receptor inhibitors in B cell malignancies. *Cancers, 12*.
Garside, P., Ingulli, E., Merica, R. R., Johnson, J. G., Noelle, R. J., & Jenkins, M. K. (1998). Visualization of specific B and T lymphocyte interactions in the lymph node. *Science, 281*, 96–99.
Iso, T., Kedes, L., & Hamamori, Y. (2003). HES and HERP families: Multiple effectors of the notch signaling pathway. *Journal of Cellular Physiology, 194*, 237–255.
Kathrein, K. L., Chari, S., & Winandy, S. (2008). Ikaros directly represses the notch target gene Hes1 in a leukemia T cell line: Implications for CD4 regulation. *Journal of Biological Chemistry, 283*, 10476–10484.
Kerfoot, S. M., Yaari, G., Patel, J. R., Johnson, K. L., Gonzalez, D. G., Kleinstein, S. H., & Haberman, A. M. (2011). Germinal center B cell and T follicular helper cell development initiates in the interfollicular zone. *Immunity, 34*, 947–960.
Lechner, M., Engleitner, T., Babushku, T., Schmidt-Supprian, M., Rad, R., Strobl, L. J., & Zimber-Strobl, U. (2021). Notch2-mediated plasticity between marginal zone and follicular B cells. *Nature Communications, 12*, 1111.
Lin, Y., Zhao, J. L., Zheng, Q. J., Jiang, X., Tian, J., Liang, S. Q., Guo, H. W., Qin, H. Y., Liang, Y. M., & Han, H. (2018). Notch signaling modulates macrophage polarization and phagocytosis through direct suppression of signal regulatory protein alpha expression. *Frontiers in Immunology, 9*, 1744.
Luzina, I. G., Atamas, S. P., Storrer, C. E., daSilva, L. C., Kelsoe, G., Papadimitriou, J. C., & Handwerger, B. S. (2001). Spontaneous formation of germinal centers in autoimmune mice. *Journal of Leukocyte Biology, 70*, 578–584.
Ma, H., Qazi, S., Ozer, Z., Zhang, J., Ishkhanian, R., & Uckun, F. M. (2013). Regulatory phosphorylation of Ikaros by Bruton's tyrosine kinase. *PLoS One, 8*, Article e71302.
Mlynarczyk, C., Fontan, L., & Melnick, A. (2019). Germinal center-derived lymphomas: The darkest side of humoral immunity. *Immunological Reviews, 288*, 214–239.
Nojima, T., Haniuda, K., Moutai, T., Matsudaira, M., Mizokawa, S., Shiratori, I., Azuma, T., & Kitamura, D. (2011). In-vitro derived germinal centre B cells differentially generate memory B or plasma cells in vivo. *Nature Communications, 2*, 465.
Okada, T., Miller, M. J., Parker, I., Krummel, M. F., Neighbors, M., Hartley, S. B., O'Garra, A., Cahalan, M. D., & Cyster, J. G. (2005). Antigen-engaged B cells undergo

chemotaxis toward the T zone and form motile conjugates with helper T cells. *PLoS Biology, 3*, e150.
Picelli, S., Faridani, O. R., Bjorklund, A. K., Winberg, G., Sagasser, S., & Sandberg, R. (2014). Full-length RNA-seq from single cells using Smart-seq2. *Nature Protocols, 9*, 171–181.
Qi, H., Cannons, J. L., Klauschen, F., Schwartzberg, P. L., & Germain, R. N. (2008). SAP-controlled T-B cell interactions underlie germinal centre formation. *Nature, 455*, 764–769.
Qi, H., Egen, J. G., Huang, A. Y., & Germain, R. N. (2006). Extrafollicular activation of lymph node B cells by antigen-bearing dendritic cells. *Science, 312*, 1672–1676.
Robinson, M. J., Ding, Z., Pitt, C., Brodie, E. J., Quast, I., Tarlinton, D. M., & Zotos, D. (2020). The amount of BCL6 in B cells shortly after antigen engagement determines their representation in subsequent germinal centers. *Cell Reports, 30*, 1530–1541. e1534.
Schwickert, T. A., Victora, G. D., Fooksman, D. R., Kamphorst, A. O., Mugnier, M. R., Gitlin, A. D., Dustin, M. L., & Nussenzweig, M. C. (2011). A dynamic T cell-limited checkpoint regulates affinity-dependent B cell entry into the germinal center. *Journal of Experimental Medicine, 208*, 1243–1252.
Shi, J., Hou, S., Fang, Q., Liu, X., Liu, X., & Qi, H. (2018). PD-1 controls follicular T helper cell positioning and function. *Immunity, 49*, 264–274 e264.
Shinnakasu, R., Inoue, T., Kometani, K., Moriyama, S., Adachi, Y., Nakayama, M., Takahashi, Y., Fukuyama, H., Okada, T., & Kurosaki, T. (2016). Regulated selection of germinal-center cells into the memory B cell compartment. *Nature Immunology, 17*, 861–869.
Song, S., & Matthias, P. D. (2018). The transcriptional regulation of germinal center formation. *Frontiers in Immunology, 9*, 2026.
Soni, C., Wong, E. B., Domeier, P. P., Khan, T. N., Satoh, T., Akira, S., & Rahman, Z. S. (2014). B cell-intrinsic TLR7 signaling is essential for the development of spontaneous germinal centers. *The Journal of Immunology, 193*, 4400–4414.
Thomas, M., Calamito, M., Srivastava, B., Maillard, I., Pear, W. S., & Allman, D. (2007). Notch activity synergizes with B-cell-receptor and CD40 signaling to enhance B-cell activation. *Blood, 109*, 3342–3350.
Victora, G. D., & Nussenzweig, M. C. (2022). Germinal centers. *Annual Review of Immunology, 40*, 413–442.
Vinuesa, C. G., Sanz, I., & Cook, M. C. (2009). Dysregulation of germinal centres in autoimmune disease. *Nature Reviews Immunology, 9*, 845–857.
Yeh, C. H., Nojima, T., Kuraoka, M., & Kelsoe, G. (2018). Germinal center entry not selection of B cells is controlled by peptide-MHCII complex density. *Nature Communications, 9*, 928.
Yoon, S. O., Zhang, X., Berner, P., Blom, B., & Choi, Y. S. (2009). Notch ligands expressed by follicular dendritic cells protect germinal center B cells from apoptosis. *The Journal of Immunology, 183*, 352–358.
Zhang, P., Zhao, Y., & Sun, X. H. (2013). Notch-regulated periphery B cell differentiation involves suppression of E protein function. *The Journal of Immunology, 191*, 726–736.
Viant, C., Wirthmiller, T., ElTanbouly, M. A., Chen, S. T., Cipolla, M., Ramos, V., … Nussenzweig, M. C. (2021). Germinal center-dependent and -independent memory B cells produced throughout the immune response. *Journal of Experimental Medicine*, 218.
Wendorff, A. A., Koch, U., Wunderlich, F. T., Wirth, S., Dubey, C., Bruning, J. C., … Radtke, F. (2010). Hes1 is a critical but context-dependent mediator of canonical Notch signaling in lymphocyte development and transformation. *Immunity, 33*, 671–684.
Zhao, M., Joy, J., Zhou, W., De, S., Wood, W. H., 3rd, Becker, K. G., … Sen, R. (2018). Transcriptional outcomes and kinetic patterning of gene expression in response to NF-kappaB activation. *PLoS Biology, 16*, Article e2006347.
Santos, M. A., Sarmento, L. M., Rebelo, M., Doce, A. A., Maillard, I., Dumortier, A., … Demengeot, J. (2007). Notch1 engagement by Delta-like-1 promotes differentiation of B lymphocytes to antibody-secreting cells. *Proceedings of the National Academy of Sciences of the United States of America, 104*, 15454–15459.
Saito, T., Chiba, S., Ichikawa, M., Kunisato, A., Asai, T., Shimizu, K., … Hirai, H. (2003). Notch2 is preferentially expressed in mature B cells and indispensable for marginal zone B lineage development. *Immunity, 18*, 675–685.